2.27-W *Q*-switched self-doubling Yb:YAB laser with controllable pulse length

Peter Dekker, Judith M. Dawes, and James A. Piper

Centre for Lasers and Applications, Macquarie University, New South Wales 2109, Australia

We report 95% conversion from the optimized *Q*-switched fundamental output to green output in the self-frequency doubling material Yb:YAB. Maximum average green powers of 2.27 W were obtained at 520–522 nm. The diode-to-green conversion efficiency was 26%. Operating at 10 kHz we obtained pulse widths ranging from 100 ns to 2 μs. The pulse duration was critically dependent on the strength of the nonlinear coupling and on the time that the acousto-optic *Q* switch was open. Numerical modeling of the system is found to predict the observed pulse-lengthening effect as well as high-average-power second-harmonic generation over a broad wavelength range.

OCIS codes: 140.3480, 140.3540, 140.3600, 190.2620.

1. INTRODUCTION

In recent years Yb-doped lasers have been developed largely as a tunable alternative to neodymium-based lasers operating in the 1-μm range.[1–5] The use of Yb^{3+} as an alternate dopant offers several advantages, including high quantum efficiency and small quantum defect, and hence reduced thermal effects. The Yb ion has a simple two-level structure, with the upper level manifold ($4f$) raised approximately 10,000 cm^{-1} from the ground state. The lower-lying laser level lies, however, within the thermally populated ground state. Hence lasers based on Yb are quasi-three-level, requiring higher pump power densities in order to overcome the deleterious effects of ground-state absorption. Furthermore, because of the simple energy level structure, Yb lasers do not exhibit any visible reabsorption, resulting in efficient intracavity doubling, where both the fundamental and the second harmonic (SH) pass through the gain material, for example, in self-doubled systems.

Previously we reported efficient cw self-doubled operation in Yb:YAB,[6] resulting in 1.1 W of green output with optimized fundamental-to-green conversions of around 26% and a diode-to-green conversion of 10%. The SH power increased quadratically with pump power, indicating low round-trip conversion. Now, in order to obtain increased intracavity intensities and hence increased conversion to the SH, we have *Q* switched the same laser, albeit at a slightly lower incident pump power.

To date, *Q*-switched operation has been reported in Yb:YAG,[7,8] Yb:S-FAP,[9] Yb:KYW,[10] Yb:KGW,[11] and Yb:YAB.[12] There are, however, limited reports of *Q*-switched intracavity doubled Yb lasers, probably because efficient extracavity doubling can be achieved with a combination of high beam quality and high peak output power. For example, Bibeau *et al.*[13] used a *Q*-switched Yb:YAG laser delivering 217-W, 30-ns pulses at 10 kHz to obtain 76 W at 515 nm when extracavity doubling using 2 KTP crystals, resulting in infrared-to-green conversion efficiencies of 35%.

An intracavity nonlinear element in a *Q*-switched laser can also be used to control the pulse length by limiting the stimulated emission rate during the output pulse interval. It has been shown[14] that pulse lengthening can be achieved at no expense to the pulse output energy, where the desired output is the SH. Pulse lengthening is obtained, in this case, owing to nonlinear conversion depleting the intracavity photon field at a rate close to the stimulated emission rate. Experimental demonstration of this technique was reported[15] with an intracavity-doubled Nd:YAG laser operating on the 946-nm transition to obtain SH pulse widths varying from 200 ns to 1 μs with approximately constant pulse energies of 0.25 mJ. The tendency of the laser to overcouple (higher nonlinear coefficient than that required to obtain peak SH power or minimum pulse width) depends critically on the ratio of the nonlinear coupling to the emission cross section of the laser material. For example, intracavity doubling of the 946-nm line in Nd:YAG as compared with the 1064-nm line requires 14 times less nonlinear coupling in order to obtain maximum peak SH power.[15] Clearly Yb lasers that have stimulated emission cross sections several orders of magnitude less than their neodymium counterparts require careful selection of any intracavity nonlinear elements if the shortest possible pulse widths are desired. This is more difficult in self-doubled systems, as there is no independent control of the gain and nonlinear media.

Q-switched self-Raman-shifted lasing was reported by Lagatsky *et al.*[11] in Yb:KGW and by Grabtchikov *et al.*[10] in Yb:KYW. In both systems the effective nonlinear coupling is small enough not to overcouple the laser. In fact Kalashnikov[16] calculated that with the addition of an intracavity stimulated Raman scattering process, pulses could be shortened by up to 1 order of magnitude if the initial saturable absorption and the *Q*-factor were controlled at both the fundamental and Raman wavelengths. Kalashnikov does not report on overcoupling or pulse lengthening, although this effect has been demonstrated by use of Raman,[17] Rayleigh,[18] and Brillouin scattering,[19] as well as two-photon absorption.[20–22]

We report here detailed experimental and numerical studies of *Q*-switched intracavity self-doubled operation of Yb:YAB. Reported SH powers are twice the powers obtained compared with cw operation[6] and approximately 1

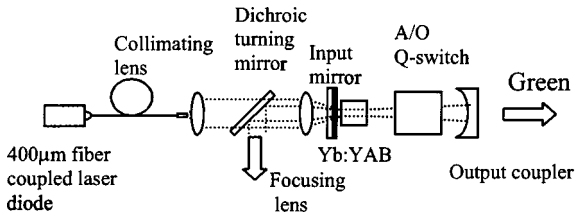

Fig. 1. Experimental setup for end-pumped Q-switched operation in Yb:YAB.

order of magnitude more power than any other diode-pumped self-doubled laser.[23,24] Through modeling of coupled-rate equations we analyze the effects of nonlinear coupling and emission cross sections on the output pulse parameters, predicting the experimental outcomes, and show high average power operation should be possible over a range of output wavelengths with varying emission cross sections.

2. EXPERIMENTS

A 10-cm hemispherical resonator, shown in Fig. 1, was used throughout the work presented here. The pump source was a 15-W fiber-coupled InGaAs diode laser (ϕ = 400 μm, NA = 0.16) operating at 977 nm. The fiber-coupled pump light was imaged onto the Yb:YAB crystal with a pair of aspheric lenses with an effective magnification of 0.55–0.74, resulting in a pump radius of 110–150 μm. An antireflection-coated 10 at.% Yb:YAB crystal (3 × 3 × 3 mm) cut for type I phase-matched operation at 1064 nm at normal incidence was used for these experiments. The crystal was held in a temperature-controlled copper block that was maintained at room temperature. The input mirror was coated high transmission at 977 nm and high reflection at 1020–1200 nm. A dichroic turning mirror was placed between the pump collimating and focusing lens both to capture the backward-propagating SH and to protect the laser diode. The cavity was completed with a 10-cm radius of curvature output coupler, whose transmission was varied 0.1%–5%. The laser-mode-to-pump-mode overlap was adjusted for a best-fit when the pump spot diameter was varied (the diode collimation and focusing position were adjusted) as well as when the cavity length was adjusted close to the stability limit for the 10-cm cavity. To obtain Q-switched operation we used an acousto-optic modulator (33027, NEOS Technologies, Florida) with an interaction length of 31 mm, a clear aperture of 2 mm, and a maximum rf drive power of 25 W.

A. Fundamental Operation

With a 2.5% output coupler with the cavity shown in Fig. 1 and operating at 10 kHz, a maximum fundamental output power of 2.39 W was obtained for 8.5 W of incident pump power. The infrared output power increased linearly with the pump power, resulting in a slope efficiency of 40%. The Yb:YAB crystal was oriented normal to the propagation direction in order to obtain minimum threshold, in this case 2.15 W incident. The laser operated at 1039–1043 nm and the pulse rise and fall times (half-max) of 33 and 56 ns, respectively, were measured. As the crystal was cut for phase matching at 1064 nm, operation at this wavelength resulted in nonoptimal SH conversion. Despite this, up to 89 mW of SH output was obtained. In comparison, with the acousto-optic Q switch removed and with the same physical cavity length of 98 mm, 3.05 W of cw IR output with 52% slope efficiency was obtained. Reduced pulse widths were obtained when the cavity lifetime was reduced (shortening the cavity length from 98 to 56 mm, the minimum possible). In this instance the pulse rise and fall times of 28 and 39 ns, respectively, were obtained. At the same time the average pulse power decreased by around 5%, owing to a reduced pump-to-cavity-mode overlap. Further reduction of the cavity lifetime (for example, an increase of the output coupler transmission) resulted in longer pulses and lower output powers. The optimal output coupler transmission at this wavelength[25] was calculated to be ~2.4%. There were no signs of pulse stretching, owing to the relatively low nonlinear coupling rate (coupling coefficient times photon density).

B. Controlling the Pulse Length

To obtain higher SH powers we used a 99.5% reflectivity output coupler. The pulse repetition frequency (prf) remained at 10 kHz. Lower prfs often resulted in coating damage, particularly when combined with high-output coupler reflectivity. To control the level of nonlinear coupling we rotated the Yb:YAB crystal in the phase-matching plane. The rotation required was approximately 0.3 deg, corresponding to a shift from the phase-matching peak to the first minima of the sinc function describing the angular detuning of the phase mismatch (the angular acceptance for phase matching to the SH near 1.06 μm is ~1.4 mrad cm). Measured IR and green output powers and pulse widths as a function of nonlinear coupling are shown in Fig. 2 (the units for nonlinear coupling are arbitrary owing to the difficulty in correlating this to the level of phase mismatch obtained when the YAB crystal is rotated; higher numbers, however, correspond to higher coupling coefficients). A maximum SH average power of 1.4 W with ~800 mW of residual IR was obtained with IR and green pulse widths of 412 and 141 ns (FWHM), respectively. When the crystal is twisted

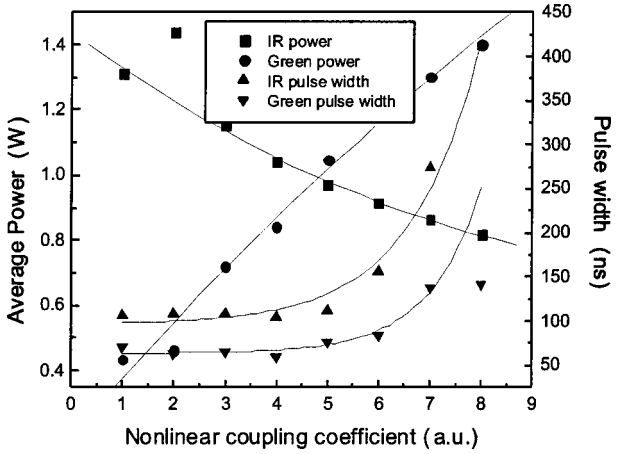

Fig. 2. Measured infrared and green average powers and pulse widths as a function of phase mismatch (higher numbers correspond to higher nonlinear coupling coefficients). Solid curves are drawn to guide the eye, 99.5% reflectivity output coupler; prf = 10 kHz

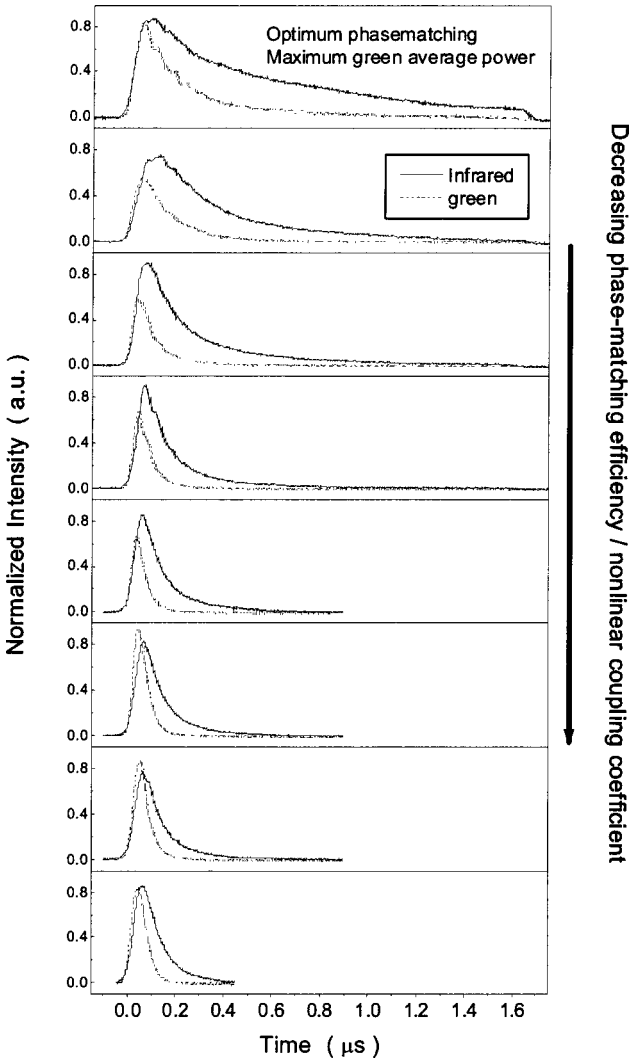

Fig. 3. Normalized infrared and green temporal outputs as a function of phase mismatch, (nonlinear coupling coefficient). (99.5% reflectivity output coupler; prf = 10 kHz).

away from optimal phase-matching, lower average SH and higher residual IR powers result. At the same time, the IR and green pulse widths (FWHM) decreased from 412 to 106 ns and from 141 to 71 ns, respectively. As shown in Fig. 3, with high nonlinear coupling rates the IR pulse shape was highly distorted, with pulse tails extending out to several microseconds. A lowering of the nonlinear coupling coefficient resulted in shorter pulses and more symmetric pulse shapes.

Peak IR powers were measured with the lowest nonlinear coupling, whereas peak green powers were obtained for intermediate coupling coefficients (in Fig. 2, peak SH power is obtained at position #5 on the abscissa). Higher coupling coefficients, however, result in higher average green powers but also in reduced peak powers owing to the stretching of the pulse. In contrast, Murray and Harris[14] calculated constant pulse energies and powers beyond optimum coupling. The difference here arises in repetitive Q switching with long lifetime materials such as Yb:YAB, allowing residual inversion to be recycled for succeeding pulses.

C. Maximizing the Second-Harmonic Output

To obtain maximum SH average power we used a high-Q cavity, and the Q-switch open time was reduced in order to counteract the effects of overcoupling. In this case the Q switch was closed before the end of the output pulse, clipping the pulse tail. Operating at 10 kHz we obtained 2.27 W of green emission at ~522 nm with 8.5-W incident pump power. The residual IR power measured 36 mW. The crystal mount temperature was 18 °C. The reported SH power included powers recorded through the output coupler (70% of total), as well as that collected through the rear dichroic. As shown in Fig. 4, the SH increased linearly with the pump power with a slope efficiency of 34%. Taking into account that the optimized infrared power also increased linearly with the pump power, we can conclude that thermally induced effects such as thermal lensing or dephasing do not strongly affect laser performance at these pump powers.

Controlling the Q-switch open time (in this case, reducing it to counteract the effects of overcoupling) resulted in more symmetric pulse shapes. When the Q switch was closed before the end of the output pulse, green powers could be increased by ~7%. The FWHM pulse width changed by only a few percent, although the full width of the output was less than one-third of the unrestricted pulse. Restriction of the output pulse duration led to an increase of the average inversion density and the average photon density, resulting in faster pulse rise times and hence more square-wave-like output. For example, the IR risetime was 40 ns when the Q switch was closed after 0.65 μs, compared with 61 ns when the Q switch was closed after 1.8 μs.

An increase in the prf decreases the energy storage time and hence reduces the initial inversion density. It is found, from the numerical analysis presented in Section 3, that this in turn requires a higher nonlinear coupling coefficient to optimize SH conversion. Consequently, the level of overcoupling is reduced for a fixed nonlinear coupling coefficient. Laser operation at higher prfs thus results in shorter pulse widths with only a small reduction in total SH power. Maximized green output power and IR and green pulse widths are shown in Fig. 5 as a function of prf. Operation at 50 kHz resulted in green powers of 1.76 W with IR and green pulse widths of 203 and 189

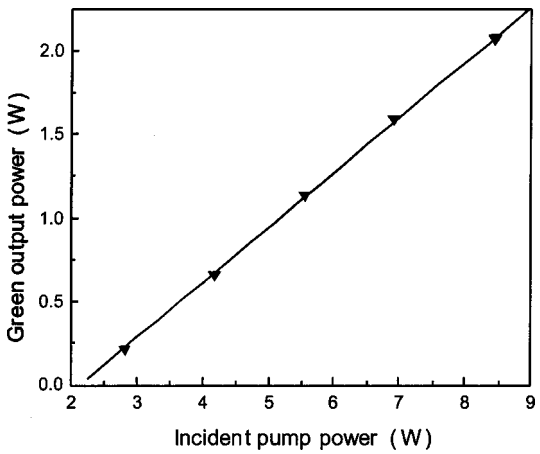

Fig. 4. Measured average green power as a function of incident pump power (including a linear fit), by use of a high-Q cavity.

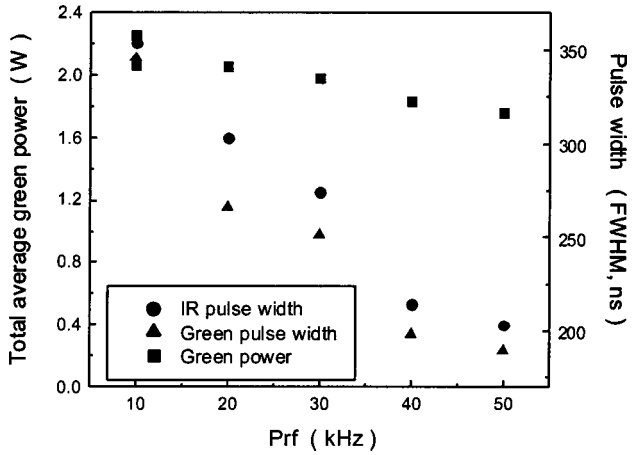

Fig. 5. Measured average green power and infrared and green pulse width as a function of pulse repetition frequency at maximum pump power (8.5 W) in a high-Q cavity.

ns, respectively. In comparison, at 20 kHz the green power increased to 2.06 W and the IR (green) pulse widths to 303 (266) ns, respectively. Operation at prfs of less than 10 kHz (in the high-Q cavity) resulted in damage to the crystal antireflective coatings.

In Q-switched operation the laser is typically operated with a bandwidth of 3–5 nm centered between 1040 and 1045 nm. The bandwidth could be reduced to 1–2 nm with a 50-μm etalon. Powers in this case dropped by at most 3%, although typically less than 1%. Unlike the cw self-doubled laser,[2] the emission spectrum varied from shot to shot (still within the quoted bandwidth), with no stable fine structure. The IR and green output was Gaussian in shape, although no beam-quality measurements were made.

3. NUMERICAL ANALYSIS

The aim of the numerical analysis presented here is to illustrate the Q-switched performance of three-level lasers, in particular repetitively Q-switched low-emission cross-section Yb systems with intracavity SH generation. The approach is based on the plane-wave model presented by Beach,[25] with an additional term included in the photon-density rate equation for the nonlinear output coupling.[26,27] For low conversion efficiencies (<20% single pass[26]) the SH is assumed to increase with the square of the fundamental.

The resulting equations are

$$\frac{\mathrm{d}n}{\mathrm{d}t} = -(f_a^e + f_b^e)c\sigma_s n\phi - \frac{n}{\tau_f}, \tag{1}$$

$$\frac{\mathrm{d}\phi}{\mathrm{d}t} = c\sigma_s n\frac{l_x}{l_c}\phi - \frac{\phi}{\tau_c} - K\phi^2, \tag{2}$$

$$K = \frac{2}{\tau_r}ch\nu\left(\frac{\mu_0}{\epsilon_0}\right)^{3/2}\frac{\omega^2 d_{\mathrm{eff}}^2 l_x^2}{(n_o^\omega)^2 n_e^{2\omega}}\mathrm{sinc}^2\left(\frac{\Delta k l_x}{2}\right). \tag{3}$$

The parameters for these equations are listed in Table 1, and c is the speed of light; μ_0 and ϵ_0 are the permeability and the permittivity of free space, respectively; and d_{eff} is the effective nonlinear coefficient in units of ampere seconds per volt squared.

Equation (1) includes loss terms from the stimulating field and those due to fluorescent decay; the pumping term is neglected, as it contributes little during the Q-switch output cycle. The loss due to fluorescent decay is insignificant during the development of the laser pulse, although it is included so that the leftover inversion can be calculated at the end of the Q-switch cycle so that any

Table 1. Key Parameters Used in the Evaluation of the Rate-Equation Model[a]

Symbol	Property	Value used in model
$h\nu$	Fundamental photon energy	1.87×10^{-19} J
ω	Fundamental frequency	1.77×10^{-15} Hz
n	Inversion density	–
ϕ	Photon density	–
σ_s	Spectroscopic cross-section	0.5×10^{-20} cm^2 at 1045 nm
f_a^e	Lower level fractional popln.	0.025 (1045 nm, 25 °C),[28]
f_b^e	Upper level fractional popln.	0.564 (25 °C)
l_x	Crystal length	0.3 cm
l_c	Cavity length	10 cm
τ_c	Cold cavity lifetime	24–260 ns
τ_r	Cavity roundtrip time	~0.7 ns
τ_f	Fluorescent lifetime	680 μs
K	Peak nonlinear coupling coefficient	7.5×10^{-9} cm^3 s^{-1}
n_o^ω	Ordinary RI at fundamental	1.75
$n_e^{2\omega}$	Extraordinary RI at SH	1.70
d_{eff}	Effective nonlinear coefficient	1.4×10^{-12} pm/V,[28] ($\times\epsilon_0$ for mks units)
$\mathrm{sinc}^2\left(\frac{\Delta k l_x}{2}\right)$	Phase mismatch	0–1 (Taken as 1 in model)

[a] Relevant material parameters are for Yb:YAB.

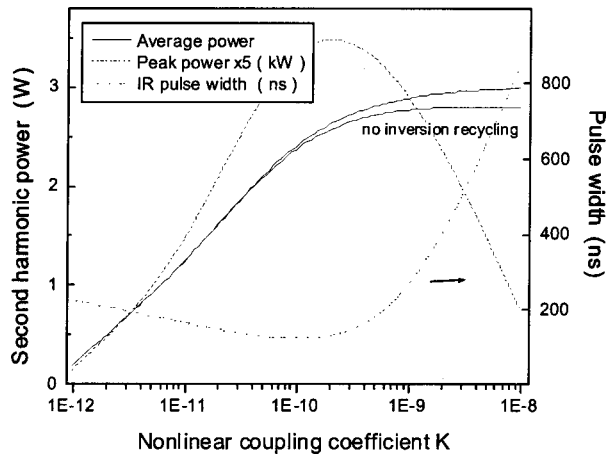

Fig. 6. Numerical calculation for average and peak green powers and infrared pulse width (FWHM) as a function of nonlinear coupling coefficient.

remaining inversion is recycled for the next pulse. This contribution has an effect only at pulse repetition rates for which the interpulse period is short compared with the fluorescent lifetime and the initial inversion is close to the threshold inversion.

The first term of Eq. (2) is due to stimulated emission increasing the intracavity photon density. High photon densities, a large emission cross section, and high inversion densities all hasten the extraction of the stored energy from the population inversion to the intracavity photon field. The second term is the infrared loss term and includes both passive (e.g., scattering and absorption losses) and output coupling losses. This term determines the rate at which photons can leak out of the cavity, in the absence of nonlinear coupling losses, and essentially puts a limit on the minimum pulse width. The third term accounts for the loss of the IR radiation coupled into its SH through the nonlinear coupling parameter K.

The magnitude of the nonlinear coupling parameter[26] K, defined in Eq. (3), is determined primarily by the effective nonlinear coefficient, crystal and cavity length, and phase mismatch. The nonlinear coupling coefficient for Yb:YAB in the experiments detailed here, ignoring phase mismatch or walk-off effects, is calculated to be $7.5 \times 10^{-9}\,\mathrm{cm}^3\,\mathrm{s}^{-1}$. The calculated nonlinear coupling coefficient is considered to be an upper bound, as it is difficult to evaluate precisely the level of phase mismatch, particularly owing to the varying center wavelength and the bandwidth of the emission.

Evaluation of Eqs. (1)–(3) was performed as a function of nonlinear coupling for Yb:YAB operating near 1045 nm in a high-Q cavity. The key parameters used in the calculation are listed in Table 1. Calculated average and peak SH powers and IR pulse widths (FWHM) are shown in Fig. 6 as a function of the nonlinear coupling coefficient. The effect of an increase of the nonlinear coupling on the laser is initially a reduction of the pulse width through an effective reduction in the cavity lifetime, and a minimum is obtained when the maximum total coupling rate is approximately half the peak stimulated emission rate; see Fig. 7. An increase of the coupling coefficient beyond this point results in increased pulse lengths, although the average coupled green power remains approximately constant. In the case of repetitive Q switching where there is leftover inversion at the end of the output pulse, higher average output powers are obtained when in the pulse-lengthening regime (this effect is more exaggerated at longer wavelengths, where the laser operates closer to threshold). The underlying influence of overcoupling on the dynamics of the laser and in particular the stimulated emission rate (SER) is shown in Fig. 7. For high coupling coefficients the SER is reduced by the removal of photons from the cavity through nonlinear conversion. The high nonlinear coupling in this case removes photons at a rate close to the SER, preventing the normal photon avalanche effect that is typically seen during Q switching.

From the analysis it can be determined that the optimal coupling coefficient for Yb:YAB operating at 1045 nm and with 8.5 W of pump is approximately $2 \times 10^{-10}\,\mathrm{cm}^3\,\mathrm{s}^{-1}$. If effects such as a reduced fundamental absorption, phase mismatch, and walk-off are ignored, the optimal coupling would be obtained with a 0.5-mm-thick nonlinear crystal. In contrast to cw systems,[28] optimal coupling is a function of pump power (initial inversion density). Higher pump powers require lower coupling coefficients; for example, a changing of the inversion ratio (ratio of inversion density to inversion density at threshold), from 4.5 (5-W pump) to 12 (8.5-W pump) changes the optimal coupling coefficient from 3.6×10^{-10} to $2 \times 10^{-10}\,\mathrm{cm}^3\,\mathrm{s}^{-1}$. This effect is also observed when the prf is changed, where higher repetition frequencies result in lower inversion ratios and hence require higher coupling coefficients in order to couple optimally.

The value of the emission cross section used in the model depends on the exact emission wavelength. Lasing at longer wavelengths generally results in lower cross

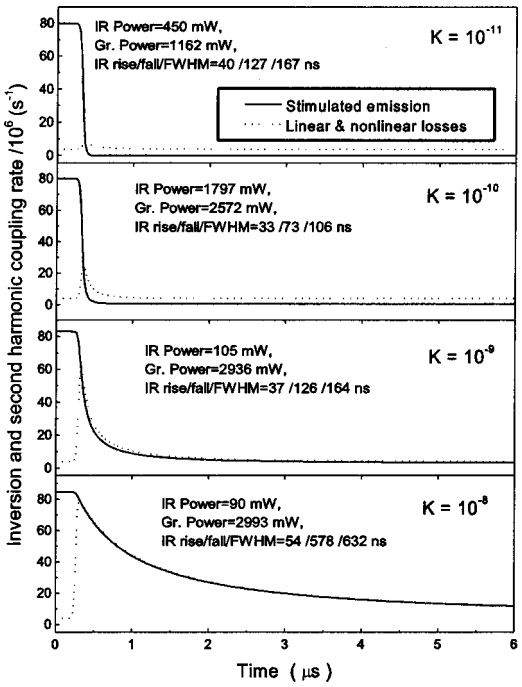

Fig. 7. Calculated stimulated emission rate and total loss (linear and nonlinear) rate as a function of time for different nonlinear coupling coefficients (K).

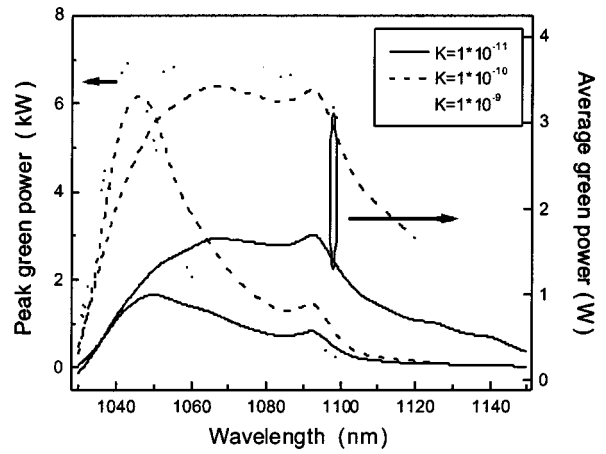

Fig. 8. Calculated peak and average green powers as a function of emission wavelength for several nonlinear coupling coefficients. (Calculated in a high-Q cavity at 10 kHz, taking into account emission cross section and lower-level fractional population).

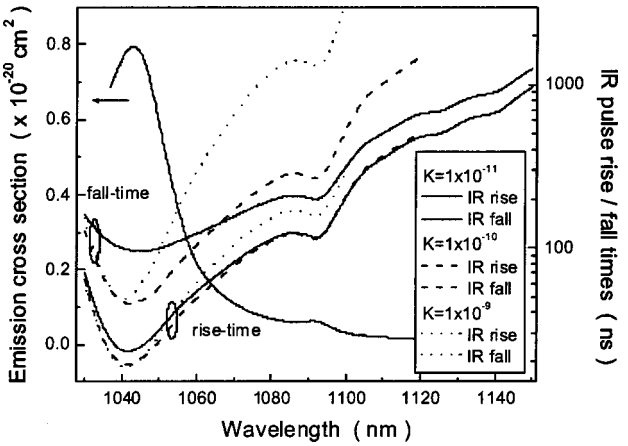

Fig. 9. Calculated infrared pulse rise and fall times (for several nonlinear coupling coefficients) and measured emission cross section as a function of wavelength. (Rise and fall times calculated in a high-Q cavity at 10 kHz, taking into account emission cross section and lower-level fractional population).

sections that in turn require lower nonlinear coefficients to couple optimally. In cw systems it has been found that when a high-Q cavity is used lasing is shifted to longer wavelengths where reabsorption losses are small and emission cross sections are low.[2] Consequently, when a high-Q cavity is used a small shift in emission wavelength is observed (~1039–1046 nm), resulting in smaller cross sections driving the laser (for fixed nonlinear coupling) further into the overcoupled regime. Calculations of peak and average green powers and fundamental pulse rise and fall times as a function of wavelength for several different nonlinear coupling coefficients are shown in Figs. 8 and 9, respectively. From the analysis it is predicted that high average power operation should be possible up to 1100 nm, although with long pulse widths. In Fig. 8 it can be seen that peak green power is obtained at shorter wavelengths (higher emission cross sections) for higher nonlinear coupling coefficients. From Fig. 9 it is observed that with a nonlinear coupling coefficient of 1×10^{-9} deviations in the pulse rise and fall times begin (as compared with $K = 1 \times 10^{-10}$) at wavelengths longer than 1042 nm, indicating overcoupling by nonlinear conversion. In this case, nonlinear conversion significantly reduces the intracavity intensity, increasing pulse rise times and slowing the SER, leading to long pulse fall times.

4. DISCUSSION

From the simple rate equation model presented in Section 3 we can see that small stimulated-emission cross sections (common for Yb materials) result in low stimulated-emission coupling rates that in turn require comparatively small nonlinear coupling coefficients in order to extract maximum peak SH power. An increase of the nonlinear coupling beyond that required to couple optimally the SH results in lower peak SH powers owing to increased pulse lengths. At the same time average green powers are found to increase beyond the optimal coupling point, in contrast to Murray and Harris,[14] owing to recycling of the leftover inversion, as the interpulse period is short compared with the fluorescence lifetime.

From the analysis and the experiment it is apparent that the required level of nonlinear coupling depends on the pulse characteristics desired. To achieve maximum peak SH power in the systems presented here, one must reduce the coupling coefficient [Eq. (3)]. This can be done through reduction of the crystal length, or (as done here) by variation of the phase mismatch (angle or temperature tuning). It is also important to note that, in comparison with Nd:LYAB[29] (with the same dimension crystal), Q-switched self-doubled operation in Yb:YAB is comparatively more efficient owing to the lower emission cross section and hence lower nonlinear coefficient required to couple optimally. In the same way, increased phase mismatch due to the broad emission (3–5 nm in Yb:YAB) is found not to reduce the infrared-to-green conversion efficiency, as the nonlinear coefficient in YAB is more than that required to couple optimally to the SH.

5. CONCLUSIONS

Q-switched SH conversion efficiencies of 95%, compared with optimized fundamental operation, have been demonstrated. Average green output powers of 2.27 W were obtained in a high-Q cavity at a prf of 10 kHz. This is more than twice the SH power obtained in cw operation and approximately 1 order of magnitude more power than the highest reported from a neodymium self-doubled system. This is an outstanding laser performance for an Yb-doped system, given that the emission cross section is significantly lower than for neodymium systems. The output power and the conversion efficiency are high, but the trade-off lies in the longer pulse widths obtained. Comparable neodymium self-doubled systems suffer, however, from deficiencies in thermal management and self-absorption that are absent here. The major factors determining the regime of operation of the laser are the emission cross section of the gain material and the nonlinear coupling parameter. When Q switched and intracavity doubled, materials with low cross sections require lower effective coupling coefficients to obtain maximum peak SH powers. Higher coupling coefficients than that

required to obtain maximum peak power results in near-constant average powers with increased pulselengths.

Such long-pulse medium-power lasers could be used as pump sources for Ti:sapphire and similar lasers, as well as for medical applications in which low-peak-power pulsed visible sources with high conversion efficiencies are required.

ACKNOWLEDGMENT

We would like to thank Richard Mildren for helpful discussions. We would also like to acknowledge the Institute of Crystal Materials Shandong University, China, for providing some of the Yb:YAB materials used in our laboratory. This research was sponsored by an Australian Research Council Large Grant.

REFERENCES

1. T. Y. Fan, S. Klunk, and G. Henein, "Diode-pumped *Q*-switched Yb:YAG laser," Opt. Lett. **18**, 423–425 (1993).
2. P. Dekker, P. A. Burns, J. M. Dawes, J. A. Piper, J. Li, X. B. Hu, and J. Y. Wang, "Widely tunable yellow-green lasers based on the self-frequency-doubling material Yb:YAB," J. Opt. Soc. Am. B **20**, 706–712 (2003).
3. V. V. Ter-Mikirtychev, M. A. Dubinskii, and V. A. Fromzel, "*Q*-switched, TEM_{00} mode, diode-pumped Yb^{3+}:YAG laser with extended tunability," Opt. Commun. **197**, 403–411 (2001).
4. S. Chenais, F. Druon, F. Balembois, G. Lucas-Leclin, P. Georges, A. Brun, M. Zavelani-Rossi, F. Auge, J. P. Chambaret, G. Aka, and D. Vivien, "Multiwatt, tunable, diode-pumped cw Yb:GdCOB laser," Appl. Phys. B **72**, 389–393 (2001).
5. A. N. P. Bustamante, D. A. Hammons, R. E. Peale, B. H. T. Chai, M. Richardson, and A. Chin, "Simultaneous cw dual-wavelength laser action and tunability performance of diode-pumped Yb^{3+}:$Sr_5(VO_4)_3F$," Opt. Commun. **192**, 309–313 (2001).
6. P. Dekker, J. M. Dawes, J. A. Piper, Y. G. Liu, and J. Y. Wang, "1.1 W CW self-frequency-doubled diode-pumped Yb:$YAl_3(BO_3)_4$ laser," Opt. Commun. **195**, 431–436 (2001).
7. E. C. Honea, R. J. Beach, S. C. Mitchell, J. A. Skidmore, M. A. Emanuel, S. B. Sutton, S. A. Payne, P. V. Avizonis, R. S. Monroe, and D. G. Harris, "High-power dual-rod Yb:YAG laser," Opt. Lett. **25**, 805–807 (2000).
8. G. D. Goodno, S. Palese, J. Harkenrider, and H. Injeyan, "Yb:YAG power oscillator with high brightness and linear polarization," Opt. Lett. **26**, 1672–1674 (2001).
9. A. J. Bayramian, C. Bibeau, R. J. Beach, C. D. Marshall, S. A. Payne, and W. F. Krupke, "Three-level *Q*-switched laser operation of ytterbium-doped $Sr_5(PO_4)_3F$ at 985 nm," Opt. Lett. **25**, 622–624 (2000).
10. A. S. Grabtchikov, A. N. Kuzmin, V. A. Lisinetskii, V. A. Orlovich, A. A. Demidovich, M. B. Danailov, H. J. Eichler, A. Bednarkiewicz, W. Strek, and A. N. Titov, "Laser operation and Raman self-frequency conversion in Yb:KYW microchip laser," Appl. Phys. B **75**, 795–797 (2002).
11. A. A. Lagatsky, A. Abdolvand, and N. V. Kuleshov, "Passive *Q* switching and self-frequency Raman conversion in a diode-pumped Yb:$KGd(WO_4)_2$ laser," Opt. Lett. **25**, 616–618 (2000).
12. P. Dekker, J. Blows, P. Wang, J. Dawes, J. Piper, Y. Liu, and J. Wang, "*Q*-switched Yb:$YAl_3(BO_3)_4$ laser in the infrared and green," in *Advanced Solid-State Lasers*, Vol. 34 of 2000 OSA Trends in Optics and Photonics Series (Optical Society of America, Washington, D.C., 2000), pp. 383–388.
13. C. Bibeau, R. J. Beach, S. C. Mitchell, M. A. Emanuel, J. Skidmore, C. A. Ebbers, S. B. Sutton, and K. S. Jancaitis, "High-average-power 1-μm performance and frequency conversion of a diode-end-pumped Yb:YAG laser," IEEE J. Quantum Electron. **34**, 2010–2019 (1998).
14. J. E. Murray and S. E. Harris, "Pulse lengthening via overcoupled internal second-harmonic generation," J. Appl. Phys. **41**, 609–613 (1970).
15. J. F. Young, J. E. Murray, R. B. Miles, and S. E. Harris, "*Q*-switched laser with controllable pulse length," Appl. Phys. Lett. **18**, 129–130 (1971).
16. V. L. Kalashnikov, "Pulse shortening in the passive *Q*-switched lasers with intracavity stimulated Raman scattering," Opt. Commun. **218**, 147–153 (2003).
17. A. Z. Grasiuk, V. F. Mulikov, and L. Csillag, "Time stretching and shaping of ruby laser giant pulses using stimulated Raman scattering," Nuovo Cimento B **64**, 300–306 (1969).
18. W. R. Callen, R. H. Pantell, and J. Warszawski, "Pulse stretching of *Q*-switched lasers," Opto-electronics **1**, 123–127 (1969).
19. S. Seidel and G. Phillipps, "Pulse lengthening by intracavity stimulated Brillouin scattering in a *Q*-switched, phase-conjugated Nd:YAG laser oscillator," Appl. Opt. **32**, 7408–7417 (1994).
20. V. A. Aleshkevich, V. V. Arsen'ev, V. S. Dneprovskii, D. N. Klyshko, and L. A. Sysoev, "Neodymium laser with regulated pulse duration," JETP Lett. **9**, 209–211 (1969).
21. A. Hordvik, "Pulse stretching utilizing two-photon induced light absorption," IEEE J. Quantum Electron. **6**, 199–203 (1970).
22. L. M. Lisitsyn, "Shaping of laser pulses with the aid of two-photon absorption in GaAs," JETP Lett. **9**, 282–284 (1969).
23. D. A. Hammons, M. Richardson, B. H. T. Chai, A. K. Chin, and R. Jollay, "Scaling of longitudinally diode-pumped self-frequency-doubling Nd:YCOB lasers," IEEE J. Quantum Electron. **36**, 991–999 (2000).
24. J. Bartschke, R. Knappe, K. J. Boller, and R. Wallenstein, "Investigation of efficient self-frequency-doubling Nd:YAB lasers," IEEE J. Quantum Electron. **33**, 2295–2300 (1997).
25. R. J. Beach, "Optimization of quasi-three level end-pumped *Q*-switched lasers," IEEE J. Quantum Electron. **31**, 1606–1613 (1995).
26. J. Liu and D. Kim, "Optimization of intracavity doubled passively *Q*-switched solid-state lasers," IEEE J. Quantum Electron. **35**, 1724–1730 (1999).
27. C. W. Wang, Y. L. Weng, P. L. Huang, H. Z. Cheng, and S. L. Huang, "Passively *Q*-switched quasi-three-level laser and its intracavity frequency doubling," Appl. Opt. **41**, 1075–1081 (2002).
28. R. G. Smith, "Theory of intracavity optical second-harmonic generation," IEEE J. Quantum Electron. **6**, 215–223 (1970).
29. P. Dekker, Y. J. Huo, J. M. Dawes, J. A. Piper, P. Wang, and B. S. Lu, "Continuous wave and *Q*-switched diode-pumped neodymium, lutetium–yttrium aluminium borate lasers," Opt. Commun. **151**, 406–412 (1998).